Quaternary Geochronology 61 (2021) 101125

Contents lists available at ScienceDirect

Quaternary Geochronology

journal homepage: http://www.elsevier.com/locate/quageo

Assessing the feasibility of the $^{228}Th/^{228}Ra$ dating method for young corals (<10 a) by gamma spectrometry

Wuhui Lin[a,b], Kefu Yu[a,b,*], Yinghui Wang[a,b,**], Xinming Liu[c], Shendong Xu[a,b], Binyuan He[c], Qiuyun Ning[c], Yinghua Li[c], Fangfang Deng[d], Jianjun Wang[e], Hao Ma[f]

[a] Coral Reef Research Center of China and School of Marine Sciences, Guangxi University, Nanning, 530004, China
[b] Guangxi Laboratory on the Study of Coral Reefs in the South China Sea, Nanning, 530004, China
[c] Guangxi Academy of Oceanography, Nanning, 530022, China
[d] Laboratory of Marine Isotopic Technology and Environmental Risk Assessment, Third Institute of Oceanography, Xiamen, 361005, China
[e] Key Laboratory of Global Change and Marine-Atmospheric Chemistry, State Oceanic Administration, Xiamen, 361005, China
[f] Department of Engineering Physics, Tsinghua University, Beijing, 100084, China

ARTICLE INFO

Keywords:
$^{228}Th/^{228}Ra$ disequilibrium
$\delta^{18}O$
Coral chronology
South China Sea
Underground laboratory
Sclerochronology

ABSTRACT

Radioactive isotopes are extremely useful for determining the age of corals, which can also provide extremely useful archives of past climate change and environmental pollution. In this study, we present a novel approach for dating young corals (<10 a), by applying the $^{228}Th/^{228}Ra$ method. $^{228}Th/^{228}Ra$ disequilibrium was widely observed in a variety of coral genera, from the fringing reefs to atoll reefs in the South China Sea using high-purity germanium γ spectrometry in an aboveground laboratory and China Jinping Underground Laboratory with the deepest carbonate rock overburden in the world. The $^{228}Th/^{228}Ra$ dating method was used to estimate the $^{228}Th/^{228}Ra$ disequilibrium-derived age based on the assumption of the ingrowth of ^{228}Th from ^{228}Ra in coral skeletons. To validate the $^{228}Th/^{228}Ra$ dating method, radiogenic ($^{228}Th/^{228}Ra$) and stable isotopes ($\delta^{18}O$) were measured for the calculations and comparison of the absolute age and relative age in *Porites* coral skeletons. The $^{228}Th/^{228}Ra$ disequilibrium-derived absolute age was found to be in agreement with the relative age based on the $\delta^{18}O$ curve. We found that the relative uncertainty of the age is simultaneously determined by the relative uncertainties of ^{228}Th and ^{228}Ra activities and $^{228}Th/^{228}Ra$ ratio, independent of the analytical methods (α spectrometry, β counter, or γ spectrometry), and is difficult to control. It was demonstrated that the dating range of the $^{228}Th/^{228}Ra$ dating method were constrained by the acceptable value of uncertainty of age. The $^{228}Th/^{228}Ra$ dating method may provide a supplementary approach to the existing coral chronological toolbox of $^{210}Pb/^{226}Ra$, ^{14}C, $^{231}Pa/^{235}U$, and $^{230}Th/^{238}U$ on a time scale from decades and hundreds of years to thousands of years.

1. Introduction

Scleractinian coral exhibit clear annual growth banding, long growth histories, wide distribution in tropical and subtropical oceans and provide valuable archives of past climate change and environmental pollution (Lough and Cooper, 2011; Yu, 2012). Determination of the absolute age of coralline material is crucial for such records and is generally based on cosmogenic or radiogenic isotope methods, such as ^{14}C, $^{210}Pb/^{226}Ra$, $^{230}Th/^{238}U$, and $^{231}Pa/^{235}U$ (Dodge and Thomson, 1974; Cobb et al., 2003; Fairbanks et al., 2005; Mortlock et al., 2005; Yu et al., 2006, 2010; Shen et al., 2008; Schmidt and Cochran, 2010; Baskaran, 2012; Clark et al., 2014). In addition, though annual cycles of density banding, Sr/Ca, Mg/Ca and $\delta^{18}O$ can provide precise floating chronologies based on sclerochronology (Yu et al., 2005a; Gillikin et al., 2019). Often, the combined use of layer-counting and isotope dating methods provides robust archives (Cobb et al., 2003; Yu et al., 2005a).

The $^{230}Th/^{238}U$ dating method is the most widely used for coralline materials spanning the last 500 000 a (Cobb et al., 2003; Yu et al., 2005b, 2012; Zhao et al., 2009). Since the first $^{230}Th/^{238}U$ dating result for fossil corals (Barnes et al., 1956), the precision and range of the

* Corresponding author. Coral Reef Research Center of China and School of Marine Sciences, Guangxi University, Nanning, 530004, China.
** Corresponding author. Coral Reef Research Center of China and School of Marine Sciences, Guangxi University, Nanning, 530004, China.
E-mail addresses: kefuyu@scsio.ac.cn (K. Yu), wyh@gxu.edu.cn (Y. Wang).

https://doi.org/10.1016/j.quageo.2020.101125
Received 16 November 2018; Received in revised form 31 August 2020; Accepted 19 September 2020
Available online 24 September 2020
1871-1014/

$^{230}Th/^{238}U$ dating method have vastly improved with the development of mass spectrometry (e.g., ICP-MS, TIMS) and sample cleaning/treatment procedures (Edwards et al., 1987; Zhao et al., 2009). The $^{230}Th/^{238}U$ dating method depends on time-consuming separation techniques and access to advance instrumentation. Such a method can be applied to young coralline materials (<10 a), however, it has been emphasized that the presence of initial ^{230}Th compromises the accuracy and precision of age determination (Cobb et al., 2003; Shen et al., 2008; Clark et al., 2012, 2014). Therefore, to obtain the ages of young corals (<10 a), we proposed the potential approach of applying the $^{228}Th/^{228}Ra$ dating method that was measured by high-purity germanium (HPGe) γ spectrometry, with the advantages of simple pre-treatment and no requirement of chemical separation.

The disequilibrium of $^{228}Th/^{228}Ra$ has been observed in seawater (Cai et al., 2002; Okubo et al., 2007; Rutgers van der Loeff et al., 2012, 2018), marine sediment (Chen and Huh, 1999), submarine hydrothermal chimneys (Reyes et al., 1995), exoskeleton of crustaceans (Bennett and Turekian, 1984; Foll et al., 1989; Reyss et al., 1996), bivalve (Turekian et al., 1975), plants (Chao et al., 2007), bone (Zinka et al., 2012), and deep-water corals (Sabatier et al., 2012). To our knowledge, application of the $^{228}Th/^{228}Ra$ dating method has not been reported for hermatypic coral skeletons from the tropical or subtropical shallow water.

The principle of the $^{228}Th/^{228}Ra$ dating method is analogous to that of the $^{230}Th/^{238}U$ dating method and is based on the ingrowth of daughter radionuclides (^{228}Th and ^{230}Th) from their grandparent radionuclides (^{228}Ra and ^{238}U, respectively), albeit with significantly different half-lives ($^{230}Th = 7.56 \times 10^4$ a (Cheng et al., 2013); $^{228}Th =$ 1.91 a (Schmidt and Cochran, 2010)). It was reported that incorporation of Th in coral skeleton is minimal (Cobb et al., 2003; Zhao et al., 2009), whereas Ra is actively taken up by corals along with other alkaline-earth metals (e.g., Ca, Sr) (Baskaran, 2012). On the basis of our understanding of Ra and Th incorporation, there is expected to be significant fractionation between ^{228}Th and ^{228}Ra at the time of coral skeleton formation. The ^{228}Th and ^{228}Ra would then be in a state of disequilibrium, which can be used to quantify the age of coral skeletons based on the extent of the ingrowth of ^{228}Th from its grandparent radionuclide ^{228}Ra. The dating range of the $^{228}Th/^{228}Ra$ dating method are constrained by the half-lives of ^{228}Th (1.91 a) and ^{228}Ra (5.75 a) and are considered to be 0–10 a (Schmidt and Cochran, 2010). Here, we explore the feasibility of applying the $^{228}Th/^{228}Ra$ dating method to modern coral skeletons.

To investigate the $^{228}Th/^{228}Ra$ disequilibrium in corals, we analysed a variety of modern coral skeletons (*Porites*, *Goniopora*, *Acropora*, *Pocillopora*, *Pachyseris*, and *Fungia*) with distinct morphologies (massive, foliaceous, branching, and solitary corals) collected from the fringing reefs in either coastal seas or atoll reefs in the open ocean of the South China Sea (SCS) using HPGe γ spectrometry located in the aboveground and deep underground laboratories. Samples were collected from 10°N to 22°N, a spatial range of >1300 km. To validate the $^{228}Th/^{228}Ra$ dating method, ages were compared with those derived along the growth axis using annual cycles of stable isotope ($\delta^{18}O$) in a *Porites* coral skeleton, the genus most often used for paleoclimate reconstructions in the tropical Indo-Pacific. The activities of ^{228}Th and ^{228}Ra are extremely low in coral skeletons and are sensitive to background radiation from cosmic rays, for this reason, some coral skeletons were measured using HPGe γ spectrometry at the China Jinping Underground Laboratory (CJPL) with the deepest carbonate rock overburden (2400 m) in the world (Cheng et al., 2017). We explored the idea of using the $^{228}Th/^{228}Ra$ dating method as a supplement to the existing coral chronology.

2. Materials and methods

2.1. Sampling and pretreatment

To verify the $^{228}Th/^{228}Ra$ disequilibrium in very recent corals, reef-building corals (length ~2 cm) were collected from (1) the fringing reefs (Luhuitou, Daya Bay, and Weizhou Island) and (2) the atoll reefs (Yongxing Island, Huangyan Island and Sanjiao Reef) in the SCS from May 2015~May 2016 (Fig. 1). These samples included massive (*Porites* and *Goniopora*), foliaceous (*Pachyseris*), branching (*Pocillopora* and *Acropora*), and solitary (*Fungia*) corals. Detailed station information and typical photos of coral genera are presented in Supplementary Data Table A1 and Fig. A1. The coral polyps were rinsed immediately after collection with deionized water to obtain modern coral skeletons and stored in a refrigerator (4 °C) before further analysis.

To compare the $^{228}Th/^{228}Ra$ dating method with band counting, a living sample of *Porites* with a maximum diameter of ~25 cm was collected from the Weizhou Island (October 2015) to provide a core with a length of 18.1 cm (Fig. 2a). This coral sample was then sliced by a water-lubricated diamond-blade masonry saw along the major growth axis to obtain a slab approximately 8 mm thick for the radiography (Fig. 2b) and $\delta^{18}O$ analysis. The coral slab was soaked and washed with deionized water to remove coral polyps before the radiography (Yu et al., 2005a).

2.2. $\delta^{18}O$ analysis in coral slab

Annual cycles of $\delta^{18}O$ along the axis of growth in WZ coral and the collection date were used to obtain the age-depth relationship. The analytical procedure of $\delta^{18}O$ in coral slab was conducted according to the previous work (Yu et al., 2005b). The dried coral slab was radiographed to guide sub-sampling for $\delta^{18}O$ analysis. Overall, this coral sample had a simple vertical growth pattern, excluding some irregular growth in the bottom layer. A length of 18.1 cm was selected for $\delta^{18}O$ and $^{228}Th/^{228}Ra$ analysis in the *Porites* coral slab (Fig. 2a).

The coral slab was soaked in 10% H_2O_2 for 24 h and washed with deionized water for 5–10 min after the radiography. This slab was ultrasonically cleaned in deionized water for 30 min to eliminate contaminants and then dried. The sub-samples (n = 367, each 1–2 mg) were drilled continuously using a high-speed rotary drill with diamond blade guided by radiography of coral slab (Fig. 2b) for $\delta^{18}O$ analysis.

Powdered carbonate was measured to obtain $\delta^{18}O$ at Guangxi University using a Finnigan MAT 253 stable isotope ratio mass spectrometer with a Fairbanks carbonate preparation device. Samples were reacted with 100% H_3PO_4 at 75 °C in an automated carbonate device to extract CO_2. All the results were reported relative to the Vienna Pee Dee Belemnite isotopic standard (V-PDB) using the GBW04405 standard ($\delta^{13}C = 0.57‰$, $\delta^{18}O = -8.49‰$). The standard deviation was approximately 0.08‰ for $\delta^{18}O$ based on repeated measurements (n = 15).

2.3. ^{228}Th and ^{228}Ra using γ spectrometry

The analytical method of ^{228}Th and ^{228}Ra using HPGe γ spectrometry located in the aboveground laboratory at Guangxi University was consistent with previous studies (Lin et al., 2018, 2019, 2020). After $\delta^{18}O$ analysis, the rest of the *Porites* core was cut perpendicular to the growth axis to provide 10 subsamples, each with a size of ~1.8 cm and mass of ~20g. For the skeletons of other coral genera, coralline materials without obvious bored and contaminated areas were selected. All samples were washed with deionized water after ultrasonic cleaning in 10% H_2O_2, dried at 60 °C, pulverized and sieved with an 80–100 mesh sieve. The powders were then transferred into a cylindrical container and sealed tightly using epoxy resin to prevent the escape of radon for a period of over 30 days (for a simultaneous measurement of ^{226}Ra) before the measurement by γ spectrometry.

2.3.1. Aboveground γ spectrometry

All samples were measured using broad-energy HPGe γ spectrometry (Canberra BE6530) with a relative efficiency of 63.4% and Genie 2000 software. The detector is surrounded in sequence by 9.5-mm stainless steel, 150-mm lead, 1-mm tin, and 1.6-mm highly pure copper to

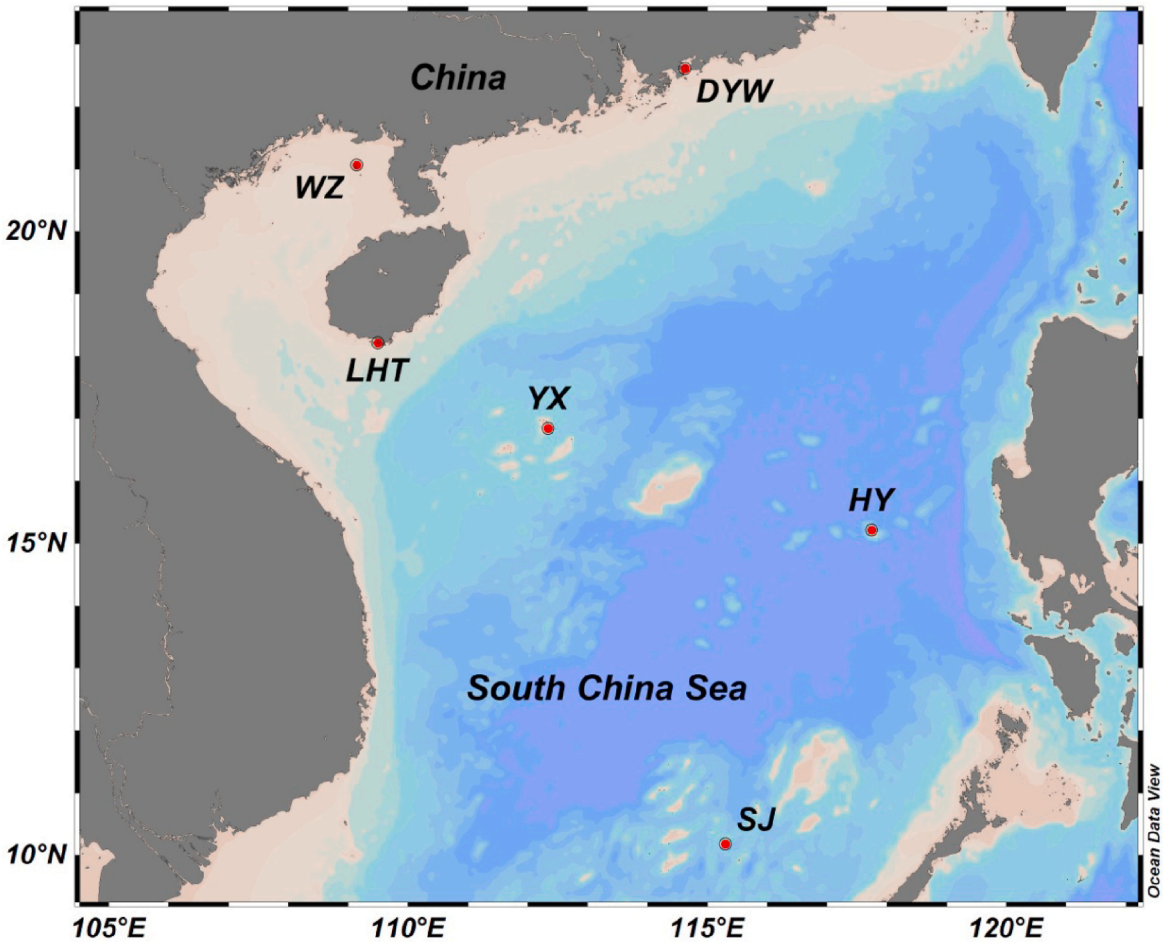

Fig. 1. Sampling stations of the Daya Bay (DYW), Weizhou Island (WZ), Luhuitou (LHT), Yongxing Island (YX), Huangyan Island (HY), and Sanjiao Reef (SJ) in the SCS.

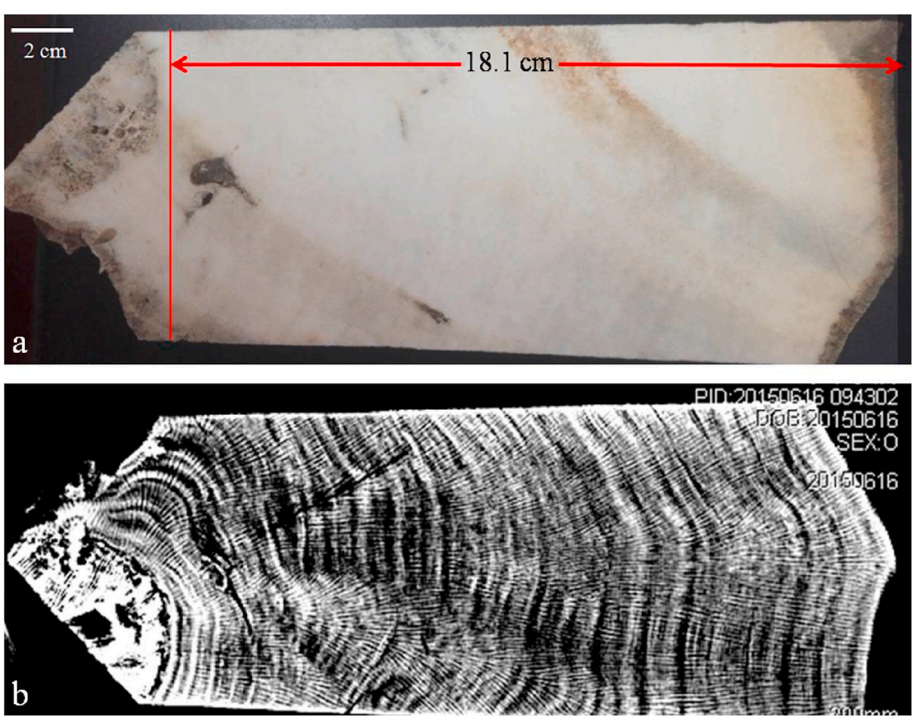

Fig. 2. *Porites* coral slab (a) and radiography image (b) from the WZ in northwestern SCS.

suppress the background. The energy resolution (FWHM) is 1.577 keV at the photopeak of 1332 keV. The relative efficiency is calibrated and cross-checked by two standard materials, the standard marine sediment from the Irish Sea (IAEA-385) and the standard river sediment (National Institute of Metrology of China GBW08304a) with a geometry identical to that of our samples.

The activities of ^{228}Th and ^{228}Ra were quantified by γ photopeaks of 583.9 keV (^{208}Tl) and 911.1 keV (^{228}Ac), respectively, with a measurement time of over 2 days for each sample. Some typical HPGe γ spectrums are presented in Supplementary Data Figure A2. The activity and its associated uncertainty at the measuring date are calculated by Eq. (1) and Eq. (2).

$$A = \frac{(n_T - n_0)}{\varepsilon m} \quad (1)$$

$$\delta A = A \times \sqrt{\frac{(n_T + n_0)}{T(n_T - n_0)^2}} \quad (2)$$

where A and δA are the activity and its associated uncertainty, respectively. n_T and n_0 are the counting rates of the sample and background, respectively. The relative efficiency ε is derived from the standard materials (GBW08304a). T is defined as the measurement time (2–4 days for each sample) of samples.

For analytical quality control, we measured the activities of radionuclides in IAEA-385 using the relative efficiency derived from the standard river sediment (GBW08304a). The obtained value was consistent with the reference value of IAEA-385 corrected to 18 April 2018 (Liu and Lin, 2018; Lin et al., 2019).

2.3.2. Underground γ spectrometry

It was recognized that the uncertainty of activity could be greatly improved using HPGe γ spectrometry located in an underground laboratory. For this reason, some typical coral skeletons were measured at the CJPL with the deepest carbonate rock overburden in the world during May 2018 (Cheng et al., 2017). The total counting rate of background radiation for HPGe γ spectrometry from the CJPL (0.027 cps) was only ~2% of that from the aboveground laboratory (1.21 cps), resulting in lower minimum detection activity and higher precision of activity. The relative uncertainties of ^{228}Th and ^{228}Ra activities at the measuring date of 2–3% were achieved at the CJPL due to the low background and long measurement time (e.g., 15, 5 and 13 days for the background, WZ-L02 and WZ-L05, respectively).

2.4. Decay/ingrowth correction

The activity of ^{232}Th is generally very low (<10^{-3} Bq/kg) in coral skeletons (Cobb et al., 2003). The activities of ^{228}Th and ^{228}Ra (1–10 Bq/kg) in our results are significantly higher than that of ^{232}Th (<10^{-3} Bq/kg) but lower than the average activities of ^{228}Th and ^{228}Ra (30 Bq/kg) in global soil and marine sediment (Lin et al., 2019, 2020). Therefore, ^{232}Th can be neglected during the decay/ingrowth correction of the ^{228}Th/^{228}Ra disequilibrium, in contrast to the ^{232}Th, which needs to be considered to estimate the initial ^{230}Th in the ^{230}Th/^{238}U dating method used in very young coral skeletons (Shen et al., 2008; Clark et al., 2012).

$$^{228}Ra \xrightarrow{T_{1/2}=5.75\ a} {}^{228}Ac \xrightarrow{T_{1/2}=6.15\ h} {}^{228}Th \xrightarrow{T_{1/2}=1.91\ a} {}^{224}Ra$$

The activities and associated uncertainties of ^{228}Th and ^{228}Ra at the measuring date were corrected to those at the sampling date according to Eqs. (3)–(6).

$$A^0_{228Ra} = A_{228Ra} \times e^{\lambda_{228Ra} \times t} \quad (3)$$

$$\delta A^0_{228Ra} = e^{\lambda_{228Ra} \times t} \times \delta A_{228Ra} \quad (4)$$

$$A^0_{228Th} = A_{228Th} \times e^{\lambda_{228Th} \times t} - \frac{\lambda_{228Th} \times A_{228Ra}}{\lambda_{228Th} - \lambda_{228Ra}} \times \left(e^{\lambda_{228Th} \times t} - e^{\lambda_{228Ra} \times t}\right) \quad (5)$$

$$\delta A^0_{228Th} = \sqrt{\left(e^{\lambda_{228Th} \times t} \times \delta A_{228Th}\right)^2 + \left[\frac{\lambda_{228Th} \times \left(e^{\lambda_{228Th} \times t} - e^{\lambda_{228Ra} \times t}\right)}{\lambda_{228Th} - \lambda_{228Ra}} \times \delta A_{228Ra}\right]^2} \quad (6)$$

where t refers to the elapsed time from the sampling date to the measuring date. A^0 and δA^0 are the activity and uncertainty at the sampling date. λ refers to the decay constant. In this study, *Porites* coral slab was collected on October 23, 2015 and measured in the aboveground laboratory during July 2017 and in the underground laboratory (CJPL) during May 2018. Therefore, the activity and uncertainty should be corrected from the measuring date to the sampling date according to Eqs. (3)–(6). Notably, the uncertainty correction of ^{228}Th activity (in radionuclide pair of ^{228}Th/^{228}Ra) has similar principles to that of ^{210}Po and ^{234}Th (in radionuclide pairs of ^{210}Po/^{210}Pb and ^{234}Th/^{238}U, respectively) and is nonlinearly amplified along with the elapsed time from the measuring date to the sampling date during the correction process according to Eq. (6) (Lin et al., 2014, 2016).

2.5. Age of modern coral skeletons

The age of coral skeletons and its uncertainty can be calculated based on activity ratio of ^{228}Th to ^{228}Ra (^{228}Th/^{228}Ra ratio) at the sampling date according to Eq. (7) and Eq. (8).

$$\tau = \frac{\ln\left(1 - \frac{A^0_{228Th}}{A^0_{228Ra}} \times \frac{\lambda_{228Th} - \lambda_{228Ra}}{\lambda_{228Th}}\right)}{\lambda_{228Ra} - \lambda_{228Th}} \quad (7)$$

$$\delta\tau = \frac{1}{\lambda_{228Th} \times \left(\frac{A^0_{228Ra}}{A^0_{228Th}} - 1\right) + \lambda_{228Ra}} \times \sqrt{\left(\frac{\delta A^0_{228Th}}{A^0_{228Th}}\right)^2 + \left(\frac{\delta A^0_{228Ra}}{A^0_{228Ra}}\right)^2} \quad (8)$$

where τ and δτ denote the age of coral skeletons and its uncertainty, respectively. The uncertainty of the calculated age is simultaneously determined by the ^{228}Th/^{228}Ra ratio and uncertainties of ^{228}Th and ^{228}Ra at the sampling date, which are propagated from uncertainties of ^{228}Th and ^{228}Ra at the measuring date according to Eq. (4) and Eq. (6).

3. Results

3.1. ^{228}Th and ^{228}Ra in distinct coral genera

The mean activities of ^{228}Th and ^{228}Ra in coral skeletons were 6.46 ± 2.46 Bq/kg and 15.00 ± 7.33 Bq/kg in the coastal ocean and 4.34 ± 2.10 Bq/kg and 5.33 ± 2.29 Bq/kg in the open ocean, respectively (Table 1). Hence, the average activity ratios of ^{228}Th to ^{228}Ra were 0.43 and 0.81 in coral skeletons from the coastal and open ocean, respectively. As the transient equilibrium value for the ^{228}Th/^{228}Ra ratio is 1.5 in a closed system (Schmidt and Cochran, 2010), the ^{228}Th/^{228}Ra ratio is significantly less than this in all modern coral skeletons from the fringing and atoll reefs, confirming the ^{228}Th/^{228}Ra disequilibrium.

3.2. ^{228}Th and ^{228}Ra in *Porites* coral slab

The ^{228}Th/^{228}Ra disequilibrium-derived ages and associated uncertainties for only the uppermost 6 sub-samples along the growth axis of the *Porites* coral core (WZ) are shown in Table 2 because the count rates of ^{228}Th and ^{228}Ra were too low for meaningful results. The age of the specific layer in *Porites* coral slab increases along with the depth of the layer (Table 2).

Table 1
Activities of ^{228}Th and ^{228}Ra, activity ratio, and age in very recent coral skeletons using γ spectrometry in the aboveground laboratory. Uncertainties are reported as one standard deviation.

Station	Genus	^{228}Th (Bq/kg)	^{228}Ra (Bq/kg)	^{228}Th/^{228}Ra	Age (a)
SJ	*Porites*	6.37 ± 1.10	9.47 ± 0.88	0.67 ± 0.13	2.46 ± 0.66
	Fungia	2.42 ± 0.98	4.23 ± 0.76	0.57 ± 0.25	1.98 ± 1.13
	Pachyseris	4.40 ± 0.79	5.15 ± 0.89	0.85 ± 0.21	3.48 ± 1.36
HY	*Porites*	4.72 ± 0.85	5.22 ± 0.76	0.90 ± 0.21	3.82 ± 1.46
	Pocillopora	2.56 ± 0.55	3.20 ± 0.50	0.80 ± 0.21	3.15 ± 1.26
	Acropora	2.28 ± 0.54	2.98 ± 0.55	0.77 ± 0.23	2.95 ± 1.29
YX	*Porites*	7.65 ± 2.87	7.09 ± 1.78	1.08 ± 0.49	5.26 ± 4.80
LHT	*Porites*	9.08 ± 2.44	11.33 ± 1.59	0.80 ± 0.24	3.16 ± 1.44
DYW	*Porites*	4.21 ± 2.75	13.25 ± 1.90	0.32 ± 0.21	0.98 ± 0.74
	Acropora	3.64 ± 0.80	8.47 ± 1.22	0.43 ± 0.11	1.40 ± 0.43
WZ	*Porites*	9.44 ± 1.73	28.95 ± 3.20	0.33 ± 0.07	1.01 ± 0.25
	Goniopora	5.35 ± 1.06	11.44 ± 0.99	0.47 ± 0.10	1.55 ± 0.40
	Acropora	7.04 ± 1.60	16.52 ± 1.62	0.43 ± 0.10	1.38 ± 0.41

Table 2
Activities of ^{228}Th and ^{228}Ra, activity ratio, and age in the *Porites* coral slab relative to the sampling date (October 23, 2015) using γ spectrometry in the aboveground laboratory. Uncertainties are reported as one standard deviation.

WZ	^{228}Th (Bq/kg)	^{228}Ra (Bq/kg)	^{228}Th/^{228}Ra ratio	Age (a)
WZ-L01	8.43 ± 2.36	24.57 ± 1.69	0.34 ± 0.09	1.07 ± 0.35
WZ-L02	10.56 ± 1.42	14.03 ± 1.01	0.75 ± 0.11	2.88 ± 0.64
WZ-L03	11.35 ± 2.62	12.31 ± 2.05	0.92 ± 0.26	3.95 ± 1.88
WZ-L04	13.89 ± 2.57	14.69 ± 1.65	0.95 ± 0.20	4.12 ± 1.53
WZ-L05	11.76 ± 2.60	9.76 ± 1.84	1.21 ± 0.35	6.75 ± 4.95
WZ-L06	9.45 ± 2.44	7.06 ± 1.70	1.34 ± 0.47	9.26 ± 12.29

3.3. Annual banding in the Porites core

Annual cycles (21 cycles) of δ^{18}O are well represented in Fig. 3. Low δ^{18}O values are observed during the summer season, consistent with results in (Yu et al., 2005a). After sampling for the ^{228}Th/^{228}Ra analysis with 10 equally spaced sub-samples across 21 cycles of δ^{18}O curve in this living *Porites* coral slab, the mean age of the outermost layer (0–1.8 cm with age range of 0–2.1 a) is calculated to be 1.05 a relative to the sampling date (October 2015). The ages of other layers could be calculated from this δ^{18}O curve and compared with the results derived from the ^{228}Th/^{228}Ra dating method. The relative uncertainty of age based on band-counting using the δ^{18}O curve was estimated to be 6.2% according to the mean extension rate and its one-sigma confidence interval (8.0 ± 0.5 mm/a) derived from radiography.

4. Discussion

4.1. ^{228}Ra in coral skeletons: coastal ocean and open ocean

We supplement the limited reported ^{228}Ra activity data for hermatypic (*Montastrea*, *Diploria*, *Solenastrea*, and *Stephanocoenia*) and deep-water coral skeletons (*Madrepora* and *Lophelia*) from the Atlantic Ocean (0.1–3 Bq/kg) with our results in Table 3 and note that activity levels are much higher in SCS (3–29 Bq/kg). The activity of ^{228}Ra in seawater, and thus, coralline material, are higher in the SCS than in other open oceans, likely because of the greater flux of ^{228}Ra from the surrounding archipelagoes (Cai et al., 2002). Higher ^{228}Ra activity in coral skeletons is reasonable to expect in the SCS after the incorporation of this high ^{228}Ra activity from seawater along with other alkaline-earth elements (e.g., Ca, Sr) into coral skeleton. Notice that coral genera were different between the SCS and Atlantic Ocean, which may contribute to the variability in the ^{228}Ra activity in distinct ocean settings.

The state of seawater in the open ocean was generally more stable than that in the coastal ocean, resulting in a stable distribution of radium in seawater in the open ocean (Henderson et al., 2013). We can make a preliminary estimate of the bioconcentration factor (BCF) for ^{228}Ra by considering the ratio between activity in coral skeleton and in seawater (Eq. (9)). The activity of ^{228}Ra in seawater was reported to be 2.5 Bq/m^3 (PA11 station) near the HY in the open ocean of the SCS (Nozaki and Yamamoto, 2001). Using the mean value for the *Porites, Pocillopora, and Acropora* from the HY station (3.80 ± 1.23 Bq/kg), we obtain a BCF for ^{228}Ra of ~1500 L/kg, which was consistent with results from the Atlantic Ocean (1300–4000 L/kg) (Baskaran, 2012). This estimate of BCF of ^{228}Ra is of the same order of magnitude as that of Ca, Sr, and U in coral skeletons (Saha et al., 2016).

$$BCF = \frac{^{228}Ra_{skeleton}}{^{228}Ra_{seawater}} \tag{9}$$

Unsurprisingly, the mean activity of ^{228}Ra in coral skeletons from the coastal ocean (15.00 ± 7.33 Bq/kg) was higher than that from the open

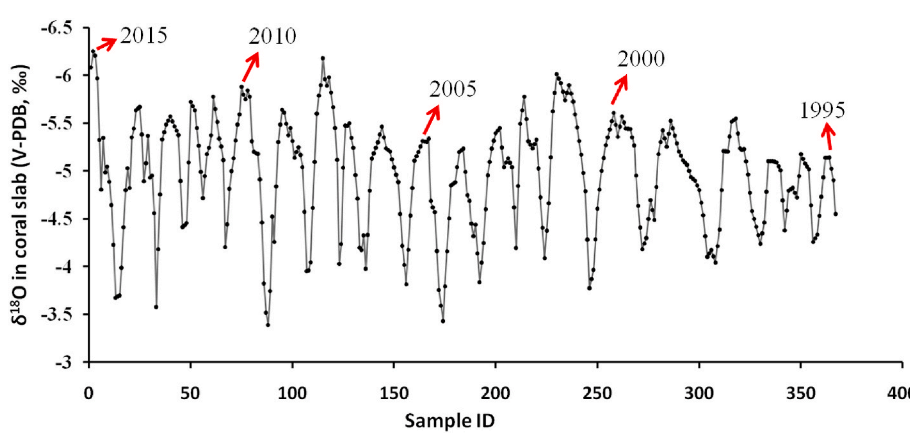

Fig. 3. δ^{18}O curve of *Porites* coral core from the WZ. Calendar years are indicated by the red arrows based on the sampling date (October 2015) and annual cycles (21 cycles) of δ^{18}O. The sample ID (n = 367) is shown in the X-axis. (For interpretation of the references to colour in this figure legend, the reader is referred to the Web version of this article.)

Table 3
^{228}Ra activity in hermatypic and deep-water coral skeletons. (Unit: Bq/kg).

Sea region	Pacific Ocean	Atlantic Ocean						
	SCS	Virgin Islands	Jamaica		Bermuda	North Carolina	Norway	
Genera		*Montastrea*	*Montastrea*	*Stephanocoenia*	*Diploria*	*Solenastrea*	*Madrepora*	*Lophelia*
^{228}Ra	3–29	0.49	0.67	0.1	0.43	0.3–3	0.1–0.26	0.1–0.7
Reference	This study	Benninger and Dodge (1986)	Dodge and Thomson (1974)	Moore and Krishnaswami (1972)	Dodge and Thomson (1974)	Moore and Krishnaswami (1972)	Sabatier et al. (2012)	Sabatier et al. (2012)

ocean (5.33 ± 2.29 Bq/kg). The consistency of ^{228}Ra activities were also observed by coral genera *Porites* and *Acropora* for the two ocean settings (Fig. 4). The same pattern is observed for ^{228}Ra activity in seawater from the SCS because of the influence of river runoff, submarine groundwater discharge, diffusion from marine sediment and water mass transit times that are long relative to the half-life of ^{228}Ra (Moore et al., 2008; Kwon et al., 2014). For example, the activity of ^{228}Ra in the coastal seawater was ~30 Bq/m^3, compared with 2–3 Bq/m^3 for the open ocean in the SCS (Nozaki and Yamamoto, 2001; Cai et al., 2002; Chen et al., 2010; Wang and Du, 2016).

4.2. ^{228}Th/^{228}Ra disequilibrium in modern coral skeleton

The ^{228}Th/^{228}Ra disequilibrium has been observed in the environment due to the different behaviors between the particle-reactive ^{228}Th and the more soluble ^{228}Ra. Although some ^{228}Th and ^{228}Ra activities have been reported for deep-water coral, the ^{228}Th/^{228}Ra dating method has not been applied (Sabatier et al., 2012). Here, we investigate ^{228}Th/^{228}Ra disequilibrium in hermatypic coral skeletons, which are widely dispersed in the tropical and subtropical oceans and are under considerable threat because of the changing ocean temperature and chemistry (Hughes et al., 2017).

We found the ^{228}Th//^{228}Ra ratio to be less than the transient equilibrium value of 1.5 expected for the closed system behaviour for coralline materials >10 a (Fig. 5). Particularly, a state of ^{228}Th/^{228}Ra disequilibrium (e.g., 0.34 for ^{228}Th/^{228}Ra ratio in WZ-L01) was observed for very recent specimens of a variety of coral genera (Table 1) and for the younger portion of a *Porites* coral slab (Table 2). The field measurement supported our assumption of the ^{228}Th/^{228}Ra disequilibrium in modern skeletons of distinct coral genera (Fig. 5).

4.3. Initial ^{228}Th

A fundamental assumption of the ^{228}Th/^{228}Ra dating method is that all measured ^{228}Th is the result of ingrowth from the decay of ^{228}Ra. However, ^{232}Th, ^{230}Th, and ^{228}Th can be partially incorporated into coral skeletons at the time of formation (Cobb et al., 2003; Shen et al., 2008; Clark et al., 2012). Initial ^{230}Th compromises the accuracy and

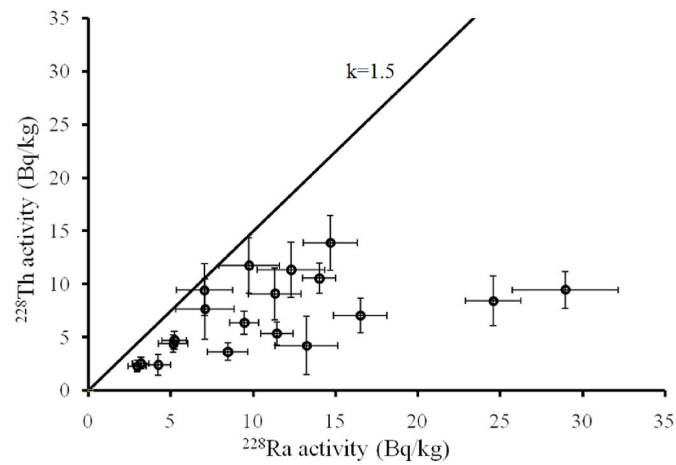

Fig. 5. Deficit of ^{228}Th to ^{228}Ra in modern coral skeleton.

precision of the ^{230}Th/^{238}U dating method for very recent corals. The same is likely to be true for the ^{228}Th/^{228}Ra dating method and needs accommodating. The degree of overestimation is determined by the initial ^{228}Th and the age of coral skeleton, as indicated in Eq. (10).

$$A^0_{228Th} = \frac{\lambda_{228Th} \times A^0_{228Ra}}{\lambda_{228Th} - \lambda_{228Ra}} \times \left[1 - e^{(\lambda_{228Ra} - \lambda_{228Th}) \times \tau}\right] + A^i_{228Th} \times e^{-\lambda_{228Th} \times \tau} \quad (10)$$

where A^i_{228Th} refers to the initial ^{228}Th.

Preliminary estimates of initial ^{228}Th in coral skeleton can be derived using estimates of the BCF for Th and ^{228}Th activity in seawater. The reported activity of ^{232}Th in seawater (10^{-3} Bq/m^3) and coral skeleton (10^{-3} Bq/kg) (e.g. (Cobb et al., 2003; Hayes et al., 2013), would suggest a BCF for Th of ~1000 L/kg. Activity of dissolved ^{228}Th was reported to be 0.1–0.5 Bq/m^3 in surface seawater in the open SCS and other open oceans (Cai et al., 2002, 2006; Okubo et al., 2007; Rutgers van der Loeff et al., 2012). The initial activity of ^{228}Th in coral skeleton is preliminarily estimated to be 0.1–0.5 Bq/kg based on the BCF for Th and

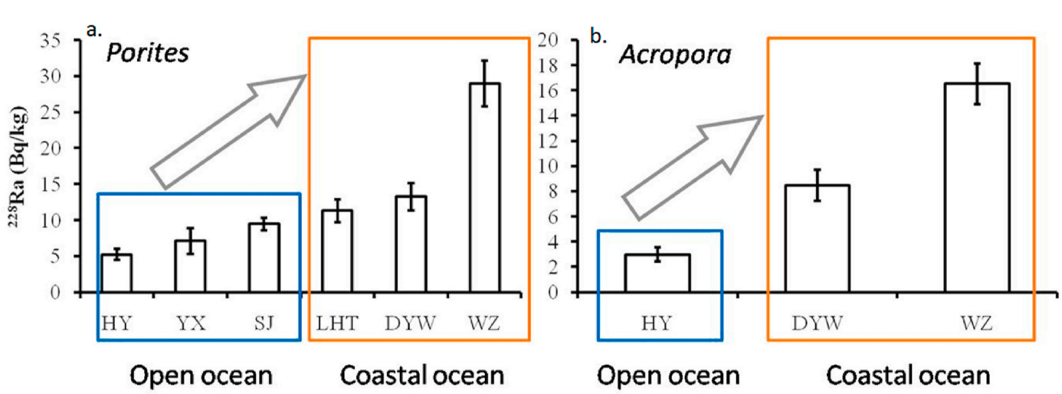

Fig. 4. Activities of ^{228}Ra in (a) *Porites* and (b) *Acropora* coral skeletons from the open ocean (blue rectangle) to the coastal sea (orange rectangle). (For interpretation of the references to colour in this figure legend, the reader is referred to the Web version of this article.)

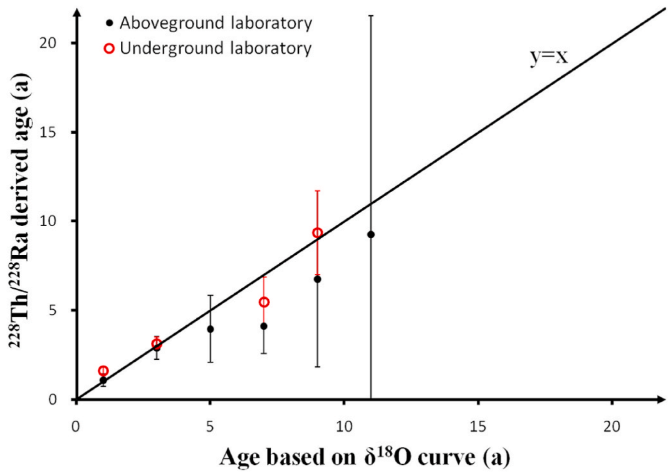

Fig. 6. Relationship between $^{228}Th/^{228}Ra$ derived age and age based on $\delta^{18}O$ curve in *Porites* coral slab. The 1:1 line is also shown.

dissolved ^{228}Th activity in seawater. The initial activity of ^{228}Th (0.1–0.5 Bq/kg) is significantly lower than the measurable ^{228}Th activity (2.0–14 Bq/kg) and is comparable to the uncertainty of ^{228}Th activity (0.5–2.4 Bq/kg) in coral skeletons (Tables 1 and 2). Also, if we consider the secular equilibrium between ^{232}Th and its progeny radionuclide, ^{228}Th, the activity of ^{228}Th would be $\sim 10^{-3}$ Bq/kg in coral skeleton and therefore negligible (Cobb et al., 2003; Clark et al., 2014). Furthermore, the contribution of initial ^{228}Th exponentially decreases along with the age of coral skeleton (the item of $A^{i}_{228Th} \times e^{-\lambda_{228Th} \times \tau}$ in Eq. (10)). It was also reported that the initial ^{228}Th was demonstrated to have very limited influence on the estimation of the transient time of seawater derived from the $^{228}Th/^{228}Ra$ disequilibrium in the Arctic Ocean (Rutgers van der Loeff et al., 2012). Therefore, the ^{228}Th activity in modern coral skeleton is mainly derived from the ingrowth of ^{228}Th from ^{228}Ra in our study. It is reasonable to neglect the initial activity of ^{228}Th to obtain the age in young coral skeletons, according to Eqs. (7) and (8).

4.4. Validation of the $^{228}Th/^{228}Ra$ dating method

On the basis of a reliable determination of ^{228}Ra activity, the observation of $^{228}Th/^{228}Ra$ disequilibrium, and the neglect of the initial ^{228}Th, the $^{228}Th/^{228}Ra$ dating method is applied to obtain the age of coral skeletons according to Eqs. (7) and (8). To validate the dating method, the $^{228}Th/^{228}Ra$ ratio and stable isotopes ($\delta^{18}O$) were measured in *Porites* coral core (Fig. 6). A comparison of $^{228}Th/^{228}Ra$ derived age and calendar age based on $\delta^{18}O$ curve and band-counting relative to the sampling date (October 23, 2015) indicates broad agreement, especially for the top three layers.

The uncertainty of age ranged from ±0.35 to ±0.64 a in the top two layers (Table 2) and is comparable to the uncertainty interval of ±0.5 to ±3.6 a in young coral skeleton (with age >3.4 a) using the $^{230}Th/^{238}U$ dating method from other studies (Clark et al., 2012, 2014; Yu et al., 2012). However, the uncertainty of age is much amplified with the increase in age for the lowermost layers of the *Porites* coral slab as the $^{228}Th/^{228}Ra$ ratio approaches transient equilibrium.

The uncertainty of $^{228}Th/^{228}Ra$ derived ages could be further reduced by increasing sample mass or improving performance of HPGe γ spectrometry (e.g., lower background of γ spectrometry). The former, however, might require reduction in sampling resolution. A lower background of γ spectrometry can take advantage of underground laboratory and use the anti-cosmic ray method for a lower minimum detection activity (Niese, 2008). Therefore, we selected some coral samples that had been analysed in the aboveground laboratory for measurement at the CJPL (Cheng et al., 2017), a facility with a very low background for γ spectrometry. Notice that the data quality at the CJPL was greatly improved (Fig. 6).

4.5. Comparative results between the aboveground laboratory and CJPL

Gamma spectrometry is widely used in the $^{228}Th/^{228}Ra$ dating method to estimate the age of plants, seawater, crustaceans, and other matrices (Kobashi and Tominaga, 1985; Foll et al., 1989; Reyes et al., 1995; Reyss et al., 1996; Chao et al., 2007; Rutgers van der Loeff et al., 2012, 2018), however, all analyses need a suitable decay correction, which can contribute to much of the uncertainty (Eq. (8)). The relative uncertainties of ages derived from the $^{228}Th/^{228}Ra$ dating method are generally in the range of 10%–50%, which are similar to our results (most 20%–50%) from the aboveground laboratory (Tables 1 and 2).

In this study, the background of HPGe γ spectrometry in the CJPL (0.027 cps) is only ~2% of that in the aboveground laboratory (1.21 cps). Comparative results from the aboveground laboratory and CJPL are represented in Table 4 and Fig. 6. The relative uncertainties of ^{228}Th and ^{228}Ra activities at the measuring date are greatly improved within the range of 2–3%, compared with 5–18% in the aboveground laboratory. The relative uncertainty of ages for WZ-L02 and WZ-L05 were significantly improved from 22% to 73% in the aboveground laboratory to 12% and 25% in the CJPL, respectively. After comparison with the results from the $\delta^{18}O$ curve (Fig. 6), the results from the CJPL showed better performance in terms of accuracy and precision of age relative to the results from the aboveground laboratory, confirming the reliability of the $^{228}Th/^{228}Ra$ dating method.

The $^{230}Th/^{238}U$ dating method was generally used to estimate the age of modern coral skeleton (Shen et al., 2008; Clark et al., 2012, 2014) and fossil coral skeleton spanning the last 500 000 a (Yu et al., 2005a; Zhao et al., 2009). However, the $^{228}Th/^{228}Ra$ dating method is suitable for very recent coral skeleton and exhibits acceptable precision and accuracy at the time scale of 0–10 a in addition to other advantages of the simple pre-treatment and no chemical separations.

The *Porites* coral generally has clear annual growth banding under radiography. The $^{228}Th/^{228}Ra$ dating method was validated in *Porites* coral skeleton by the combination of the $\delta^{18}O$ curve and radiography in this study. However, the annual growth banding cannot be well

Table 4
Comparison of ^{228}Th activity, ^{228}Ra activity, and age derived from the $^{228}Th/^{228}Ra$ dating method in *Porites* coral slab using HPGe-γ spectrometry from the CJPL and aboveground laboratory. The age based on the $\delta^{18}O$ curve is also represented for comparison. Uncertainties are reported as one standard deviation.

WZ	Results from the aboveground laboratory					Results from the CJPL					Result from ^{18}O
	Activity at measuring date (July 2017)		Activity at sampling date (October 2015)		Age	Activity at measuring date (May 2018)		Activity at sampling date (October 2015)		Age	Age
	^{228}Th	^{228}Ra	^{228}Th	^{228}Ra		^{228}Th	^{228}Ra	^{228}Th	^{228}Ra		
WZ-L02	11.47 ± 0.64	11.42 ± 0.82	10.56 ± 1.42	14.03 ± 1.01	2.88 ± 0.64	9.67 ± 0.22	8.66 ± 0.24	9.34 ± 0.69	11.73 ± 0.32	3.13 ± 0.37	3.05 ± 0.19
WZ-L05	10.36 ± 1.18	7.94 ± 1.49	11.76 ± 2.60	9.76 ± 1.84	6.75 ± 4.95	6.81 ± 0.17	4.82 ± 0.16	8.76 ± 0.50	6.53 ± 0.22	9.35 ± 2.37	9.05 ± 0.56

identified in the skeletons of other coral genera, such as solitary and foliaceous corals (e.g., *Fungia, Pachyseris*). On the basis of similar mechanisms of coral calcification, the age of these coral genera without clear growth banding can be estimated by the $^{228}Th/^{228}Ra$ dating method.

4.6. Uncertainty propagation in the $^{228}Th/^{228}Ra$ dating method

The uncertainty of age is a key parameter for obtaining high-quality results, however, it has been rarely discussed in detail (Reyes et al., 1995; Reyss et al., 1996; Chao et al., 2007; Rutgers van der Loeff et al., 2012; Zinka et al., 2012). In this study, we utilize the relative uncertainty of age ($\delta\tau/\tau$) to analyze the precision of age according to Eq. (11) after the substitution of Eq. (7) and Eq. (8). The relative uncertainty of age is simultaneously determined by the $^{228}Th/^{228}Ra$ ratio and the relative uncertainties of ^{228}Th and ^{228}Ra activities at the sampling date.

$$\text{Relative uncertainty of age} = \frac{\delta\tau}{\tau} = \frac{(\lambda_{228Ra} - \lambda_{228Th}) \times \sqrt{\left(\frac{\delta A^0_{228Th}}{A^0_{228Th}}\right)^2 + \left(\frac{\delta A^0_{228Ra}}{A^0_{228Ra}}\right)^2}}{\left[\lambda_{228Th} \times \left(\frac{A^0_{228Ra}}{A^0_{228Th}} - 1\right) + \lambda_{228Ra}\right] \times \ln\left(1 - \frac{A^0_{228Th}}{A^0_{228Ra}} \times \frac{\lambda_{228Th} - \lambda_{228Ra}}{\lambda_{228Th}}\right)} \quad (11)$$

Notice that the relative uncertainty of ^{228}Th and ^{228}Ra at the sampling date could be well regulated to reduce $\delta\tau/\tau$ by lengthening the measurement time, increasing the sample mass, and decreasing the background of γ spectrometry. However, the value of $\delta\tau/\tau$ is also affected by $^{228}Th/^{228}Ra$ ratio, which is independent of the analytical methods (α spectrometry, β counter, or γ spectrometry) and is difficult to control. For example, although the relative uncertainty of ^{228}Th and ^{228}Ra at the measuring date was well regulated within the range of 2–3% at the CJPL (in Table 4), the relative uncertainty of calculated age was amplified to be 25.3% for WZ-L05 (with the $^{228}Th/^{228}Ra$ ratio and age of 1.34 and 9.35 a, respectively, in Table 4).

Therefore, the theoretical analysis of Eq. (11) is illustrated to evaluate the impacts of the $^{228}Th/^{228}Ra$ ratio and the relative uncertainties of the ^{228}Th and ^{228}Ra activities at the sampling date on the relative uncertainty of age (Fig. 7). Overall, the relative uncertainty of age is proportional to the $^{228}Th/^{228}Ra$ ratio and the relative uncertainty of ^{228}Th and ^{228}Ra activities at the sampling date (k in the legend of Fig. 7).

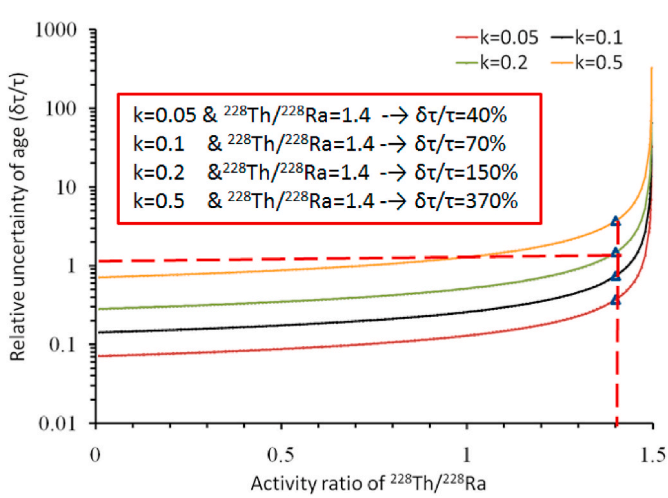

Fig. 7. Relative uncertainty of age as a function of the activity ratio of $^{228}Th/^{228}Ra$ and relative uncertainty of the ^{228}Th and ^{228}Ra activities (k).

It is noted that the relative uncertainty of age is rapidly amplified when $^{228}Th/^{228}Ra$ ratio is > 1.4 (e.g., 370% for $\delta\tau/\tau$ in the legend of Fig. 7). Therefore, the precision of the $^{228}Th/^{228}Ra$ disequilibrium-derived age is not suitable for quantitative analysis when activity ratio of $^{228}Th/^{228}Ra$ is > 1.4 with an equivalent age of 11.3 a for coral skeleton according to Eq. (7). The acceptable value of the precision of the $^{228}Th/^{228}Ra$ disequilibrium-derived age will ultimately constrain the dating range of the $^{228}Th/^{228}Ra$ dating method after uncertainty propagation from counting statistics of ^{228}Th and ^{228}Ra at the measuring date to uncertainty of age.

5. Conclusion

In the present study, we explored the feasibility of the $^{228}Th/^{228}Ra$ dating method based on the reliable determination of ^{228}Ra activity, the observation of $^{228}Th/^{228}Ra$ disequilibrium in very recent coral skeletons, and the assumption of a negligible initial ^{228}Th. A decline in ^{228}Ra activity of modern coral skeleton from the coastal ocean to the open ocean was observed and attributed to the short half-life of ^{228}Ra (5.75 a) relative to long transient time of water mass from the coastal ocean to the open ocean. We found that the $^{228}Th/^{228}Ra$ disequilibrium was observed in coral skeletons from the SCS with a range of morphologies (e.g., massive, branching, solitary corals) from the fringing reefs in the coastal ocean to the atoll reefs in the open ocean, with a latitude spanning from 10°N to 22°N. The initial ^{228}Th is considered to have a negligible influence on the $^{228}Th/^{228}Ra$ disequilibrium-derived age.

To validate the $^{228}Th/^{228}Ra$ dating method, calendar ages were determined by annual band-counting using $\delta^{18}O$ in *Porites* coral and compared with HPGe γ spectrometric results from an aboveground laboratory and underground facility at CJPL (with an extremely low background). Reasonable agreement was observed for ages up to ~6 a and we considered it feasible to extend this to 10 a with improved background, longer count times and further consideration of initial ^{228}Th. The $^{228}Th/^{228}Ra$ dating method has a simple pre-treatment, no chemical separation, good precision and accuracy, and a wide application for a variety of coral genera including those without clear growth banding. The successful application of the $^{228}Th/^{228}Ra$ dating method in living coral skeleton may also benefit the age determination of recently dead coral skeleton and new invasive reef-building coral in remote sea areas without direct time-series observations of corals. This is significant for identifying potential drivers in the context of climate change and anthropogenic activity.

Data availability

All the data excluding $\delta^{18}O$ are presented in the manuscript. The $\delta^{18}O$ data are available in the Supplementary Materials.

Declaration of competing interest

The authors declare that they have no known competing financial interests or personal relationships that could have appeared to influence the work reported in this paper.

Acknowledgements

We are grateful for the suggestions and comments by Dr. David A. Richards and three reviewers. This study was financially supported by the National Natural Science Foundation of China (41906043) and the Natural Science Foundation of Guangxi Province (2019GXNSFAA185006, 2017GXNSFBA198096, AA17129063 and AA17204074). The authors declare no competing financial interests.

Appendix A. Supplementary data

Supplementary data to this article can be found online at https://doi.org/10.1016/j.quageo.2020.101125.

References

Barnes, J.W., Lang, E.J., Potratz, H.A., 1956. Ratio of ionium to uranium in coral limestone. Science 124 (3213), 175.
Baskaran, M., 2012. Dating of biogenic and inorganic carbonates using ^{210}Pb-^{226}Ra disequilibrium method: a review. In: Baskaran, M. (Ed.), Handbook of Environmental Isotope Geochemistry, vol. I. Springer Berlin Heidelberg, Berlin, Heidelberg, pp. 789–809.
Bennett, J.T., Turekian, K.K., 1984. Radiometric ages of Brachyuran crabs from the galapagos spreading-center hydrothermal ventfield. Limnol. Oceanogr. 29 (5), 1088–1091.
Benninger, L.K., Dodge, R.E., 1986. Fallout plutonium and natural radionuclides in annual bands of the coral Montastrea annularis, St. Croix, US Virgin Islands. Geochem. Cosmochim. Acta 50 (12), 2785–2797.
Cai, P., Dai, M., Chen, W., Tang, T., Zhou, K., 2006. On the importance of the decay of ^{234}Th in determining size-fractionated C/^{234}Th ratio on marine particles. Geophys. Res. Lett. 33 (23), 160–176.
Cai, P., Huang, Y., Chen, M., Guo, L., Liu, G., Qiu, Y., 2002. New production based on ^{228}Ra-derived nutrient budgets and thorium-estimated POC export at the intercalibration station in the South China Sea. Deep Sea Res. Oceanogr. Res. Pap. 49 (1), 53–66.
Chao, J.H., Niu, H., Chiu, C.Y., Lin, C., 2007. A potential dating technique using ^{228}Th/^{228}Ra ratio for tracing the chronosequence of elemental concentrations in plants. Appl. Radiat. Isot. 65 (6), 641–648.
Chen, H.Y., Huh, C.A., 1999. ^{232}Th–^{228}Ra–^{228}Th disequilibrium in East China Sea sediments. J. Environ. Radioact. 42 (1), 93–100.
Chen, W., Liu, Q., Huh, C.A., Dai, M., Miao, Y.C., 2010. Signature of the Mekong River plume in the western South China Sea revealed by radium isotopes. J. Geophys. Res.: Oceans 115 (C12).
Cheng, H., Lawrence Edwards, R., Shen, C.-C., Polyak, V.J., Asmerom, Y., Woodhead, J., Hellstrom, J., Wang, Y., Kong, X., Spötl, C., Wang, X., Calvin Alexander, E., 2013. Improvements in ^{230}Th dating, ^{230}Th and ^{234}U half-life values, and U–Th isotopic measurements by multi-collector inductively coupled plasma mass spectrometry. Earth Planet Sci. Lett. 371–372, 82–91.
Cheng, J.-P., Kang, K.-J., Li, J.-M., Li, J., Li, Y.-J., Yue, Q., Zeng, Z., Chen, Y.-H., Wu, S.-Y., Ji, X.-D., Wong, H.T., 2017. The China jinping underground laboratory and its early science. Annu. Rev. Nucl. Part Sci. 67 (1), 231–251.
Clark, T.R., Roff, G., Zhao, J.X., Feng, Y.X., Done, T.J., Pandolfi, J.M., 2014. Testing the precision and accuracy of the U–Th chronometer for dating coral mortality events in the last 100 years. Quat. Geochronol. 23 (10), 35–45.
Clark, T.R., Zhao, J.-x., Feng, Y.-x., Done, T.J., Jupiter, S., Lough, J., Pandolfi, J.M., 2012. Spatial variability of initial ^{230}Th/^{232}Th in modern Porites from the inshore region of the Great Barrier Reef. Geochem. Cosmochim. Acta 78 (Suppl. C), 99–118.
Cobb, K.M., Charles, C.D., Cheng, H., Kastner, M., Edwards, R.L., 2003. U/Th-dating living and young fossil corals from the central tropical Pacific. Earth Planet Sci. Lett. 210 (1), 91–103.
Dodge, R.E., Thomson, J., 1974. The natural radiochemical and growth records in contemporary hermatypic corals from the Atlantic and Caribbean. Earth Planet Sci. Lett. 23 (3), 313–322.
Edwards, L.R., Chen, J.H., Wasserburg, G.J., 1987. ^{238}U-^{234}U-^{230}Th-^{232}Th systematics and the precise measurement of time over the past 500,000 years. Earth Planet Sci. Lett. 81 (2), 175–192.
Fairbanks, R.G., Mortlock, R.A., Chiu, T.-C., Cao, L., Kaplan, A., Guilderson, T.P., Fairbanks, T.W., Bloom, A.L., Grootes, P.M., Nadeau, M.-J., 2005. Radiocarbon calibration curve spanning 0 to 50,000 years BP based on paired ^{230}Th/^{234}U/^{238}U and ^{14}C dates on pristine corals. Quat. Sci. Rev. 24 (16), 1781–1796.
Foll, D.L., Brichet, E., Reyss, J.L., Lalou, C., Latrouite, D., 1989. Age determination of the spider crab maja squinado and the European lobster Homarus gammarus by ^{228}Th/^{228}Ra chronology: possible extension to other Crustaceans. Can. J. Fish. Aquat. Sci. 46 (4), 720–724.
Gillikin, D.P., Wanamaker, A.D., Andrus, C.F.T., 2019. Chemical sclerochronology. Chem. Geol. 526, 1–6.
Hayes, C.T., Anderson, R.F., Fleisher, M.Q., Serno, S., Winckler, G., Gersonde, R., 2013. Quantifying lithogenic inputs to the North Pacific Ocean using the long-lived thorium isotopes. Earth Planet Sci. Lett. 383 (383), 16–25.
Henderson, P.B., Morris, P.J., Moore, W.S., Charette, M.A., 2013. Methodological advances for measuring low-level radium isotopes in seawater. J. Radioanal. Nucl. Chem. 296 (1), 357–362.
Hughes, T.P., Kerry, J.T., Álvarez-Noriega, M., Álvarez-Romero, J.G., Anderson, K.D., Baird, A.H., Babcock, R.C., Beger, M., Bellwood, D.R., Berkelmans, R., Bridge, T.C., Butler, I.R., Byrne, M., Cantin, N.E., Comeau, S., Connolly, S.R., Cumming, G.S., Dalton, S.J., Diaz-Pulido, G., Eakin, C.M., Figueira, W.F., Gilmour, J.P., Harrison, H. B., Heron, S.F., Hoey, A.S., Hobbs, J.-P.A., Hoogenboom, M.O., Kennedy, E.V., Kuo, C.-y., Lough, J.M., Lowe, R.J., Liu, G., McCulloch, M.T., Malcolm, H.A., McWilliam, M.J., Pandolfi, J.M., Pears, R.J., Pratchett, M.S., Schoepf, V., Simpson, T., Skirving, W.J., Sommer, B., Torda, G., Wachenfeld, D.R., Willis, B.L., Wilson, S.K., 2017. Global warming and recurrent mass bleaching of corals. Nature 543 (7645), 373–377.
Kobashi, A., Tominaga, T., 1985. ^{228}Ra-^{228}Th dating of plant samples. Int. J. Appl. Radiat. Isot. 36, 547–553.
Kwon, E.Y., Kim, G., Primeau, F., Moore, W.S., Cho, H.M., Devries, T., Sarmiento, J.L., Charette, M.A., Cho, Y.K., 2014. Global estimate of submarine groundwater discharge based on an observationally constrained radium isotope model. Geophys. Res. Lett. 41 (23), 8438–8444.
Lin, W., Chen, L., Zeng, S., Li, T., Wang, Y., Yu, K., 2016. Residual β activity of particulate ^{234}Th as a novel proxy for tracking sediment resuspension in the ocean. Sci. Rep. 6, 27069.
Lin, W., Feng, Y., Yu, K., Lan, W., Wang, Y., Mo, Z., Ning, Q., Feng, L., He, X., Huang, Y., 2020. Long-lived radionuclides in marine sediments from the Beibu Gulf, South China Sea: spatial distribution, controlling factors, and proxy for transport pathway. Mar. Geol. 424, 106157.
Lin, W., Ma, H., Chen, L., Zeng, Z., He, J., Zeng, S., 2014. Decay/ingrowth uncertainty correction of ^{210}Po/^{210}Pb in seawater. J. Environ. Radioact. 137, 22–30.
Lin, W., Yu, K., Wang, Y., Liu, X., Ning, Q., Huang, X., 2019. Radioactive level of coral reefs in the South China Sea. Mar. Pollut. Bull. 142, 43–53.
Lin, W., Yu, K., Wang, Y., Liu, X., Wang, J., Ning, Q., Li, Y., 2018. Extremely low radioactivity in marine sediment of coral reefs and its mechanism. Chin. Sci. Bull. 63 (21), 2173–2183 (In Chinese).
Liu, X., Lin, W., 2018. Natural radioactivity in the beach sand and soil along the coastline of Guangxi Province, China. Mar. Pollut. Bull. 135, 446–450.
Lough, J.M., Cooper, T.F., 2011. New insights from coral growth band studies in an era of rapid environmental change. Earth Sci. Rev. 108 (3), 170–184.
Moore, W.S., Krishnaswami, S., 1972. Coral growth rates using ^{228}Ra and ^{210}Pb. Earth Planet Sci. Lett. 15 (2), 187–190.
Moore, W.S., Sarmiento, J.L., Key, R.M., 2008. Submarine groundwater discharge revealed by ^{228}Ra distribution in the upper Atlantic Ocean. Nat. Geosci. 1 (5), 309–311.
Mortlock, R.A., Fairbanks, R.G., Chiu, T.-c., Rubenstone, J., 2005. ^{230}Th/^{234}U/^{238}U and ^{231}Pa/^{235}U ages from a single fossil coral fragment by multi-collector magnetic-sector inductively coupled plasma mass spectrometry. Geochem. Cosmochim. Acta 69 (3), 649–657.
Niese, S., 2008. Underground laboratories for low-level radioactivity measurements. In: Povinec, P.P. (Ed.), Radioactivity in the Environment, vol. 11. Elsevier., pp. 209–239
Nozaki, Y., Yamamoto, Y., 2001. Radium-228 based nitrate fluxes in the eastern Indian Ocean and the South China Sea and a silicon-induced "alkalinity pump" hypothesis. Global Biogeochem. Cycles 15 (3), 555–567.
Okubo, A., Obata, H., Luo, S., Gamo, T., Yamamoto, Y., Minami, H., Yamada, M., 2007. Particle flux in the twilight zone of the eastern Indian Ocean: a constraint from ^{234}U–^{230}Th and ^{228}Ra–^{228}Th disequilibria. Deep Sea Res. Oceanogr. Res. Pap. 54 (10), 1758–1772.
Reyes, A.O., Moore, W.S., Stakes, D.S., 1995. ^{228}Th/^{228}Ra ages of a barite-rich chimney from the endeavour segment of the juan de Fuca ridge. Earth Planet Sci. Lett. 131 (1), 99–113.
Reyss, J.L., Schmidt, S., Latrouite, D., Floris, S., 1996. Age determination of crustacean carapaces using ^{228}Th/^{228}Ra measurements by ultra low level gamma spectroscopy. Appl. Radiat. Isot. 47 (9), 1049–1053.
Rutgers van der Loeff, M., Cai, P., Stimac, I., Bauch, D., Hanfland, C., Roeske, T., Moran, S.B., 2012. Shelf-basin exchange times of Arctic surface waters estimated from ^{228}Th/^{228}Ra disequilibrium. J. Geophys. Res.: Oceans 117 (C3), C03024.
Rutgers van der Loeff, M., Kipp, L., Charette, M.A., Moore, W.S., Black, E., Stimac, I., Charkin, A., Bauch, D., Valk, O., Karcher, M., Krumpen, T., Casacuberta, N., Smethie, W., Rember, R., 2018. Radium isotopes across the Arctic Ocean show time scales of water mass ventilation and increasing shelf inputs. J. Geophys. Res.: Oceans 123, 4853–4873.
Sabatier, P., Reyss, J.-L., Hall-Spencer, J.M., Colin, C., Frank, N., Tisnerat-Laborde, N., Bordier, L., Douville, E., 2012. ^{210}Pb-^{226}Ra chronology reveals rapid growth rate of Madrepora oculata and Lophelia pertusa on world's largest cold-water coral reef. Biogeosciences 9 (3), 1253–1265.
Saha, N., Webb, G.E., Zhao, J.-X., 2016. Coral skeletal geochemistry as a monitor of inshore water quality. Sci. Total Environ. 566, 652–684.
Schmidt, S., Cochran, J.K., 2010. Radium and radium-daughter nuclides in carbonates: a brief overview of strategies for determining chronologies. J. Environ. Radioact. 101 (7), 530–537.
Shen, C.-C., Li, K.-S., Sieh, K., Natawidjaja, D., Cheng, H., Wang, X., Edwards, R.L., Lam, D.D., Hsieh, Y.-T., Fan, T.-Y., 2008. Variation of initial ^{230}Th/^{232}Th and limits of high precision U–Th dating of shallow-water corals. Geochem. Cosmochim. Acta 72 (17), 4201–4223.
Turekian, K.K., Cochran, J.K., Kharkar, D.P., Cerrato, R.M., Vaisnys, J.R., Sanders, H.L., Grassle, J.F., Allen, J.A., 1975. Slow growth rate of a deep-sea clam determined by ^{228}Ra chronology. Proc. Natl. Acad. Sci. U. S. A 72 (7), 2829–2832.

Wang, X., Du, J., 2016. Submarine groundwater discharge into typical tropical lagoons: a case study in eastern Hainan Island, China. G-cubed 17 (11), 4366–4382.

Yu, K.-F., Zhao, J.-X., Shi, Q., Chen, T.-G., Wang, P.-X., Collerson, K.D., Liu, T.-S., 2006. U-series dating of dead Porites corals in the South China sea: evidence for episodic coral mortality over the past two centuries. Quat. Geochronol. 1 (2), 129–141.

Yu, K.-F., Zhao, J.-X., Wei, G.-J., Cheng, X.-R., Chen, T.-G., Felis, T., Wang, P.-X., Liu, T.-S., 2005a. $\delta^{18}O$, Sr/Ca and Mg/Ca records of Porites lutea corals from Leizhou Peninsula, northern South China Sea, and their applicability as paleoclimatic indicators. Palaeogeogr. Palaeoclimatol. Palaeoecol. 218 (1), 57–73.

Yu, K., Hua, Q., Zhao, J.X., Hodge, E., Fink, D., Barbetti, M., 2010. Holocene marine ^{14}C reservoir age variability: evidence from ^{230}Th-dated corals in the South China Sea. Paleoceanography 25, 375–387.

Yu, K., Zhao, J., Roff, G., Lybolt, M., Feng, Y., Clark, T., Li, S., 2012. High-precision U-series ages of transported coral blocks on Heron Reef (southern Great Barrier Reef) and storm activity during the past century. Palaeogeogr. Palaeoclimatol. Palaeoecol. 337–338 (2), 23–36.

Yu, K.F., 2012. Coral reefs in the South China Sea: their response to and records on past environmental changes. Sci. China Earth Sci. 55 (8), 1217–1229.

Yu, K.F., Zhao, J.X., Wei, G.J., Cheng, X.R., Wang, P.X., 2005b. Mid–late Holocene monsoon climate retrieved from seasonal Sr/Ca and $\delta^{18}O$ records of Porites lutea corals at Leizhou Peninsula, northern coast of South China Sea. Global Planet. Change 47 (2–4), 301–316.

Zhao, J., Yu, K., Feng, Y., 2009. High-precision ^{238}U-^{234}U-^{230}Th disequilibrium dating of the recent past: a review. Quat. Geochronol. 4 (5), 423–433.

Zinka, B., Kandlbinder, R., Schupfner, R., Haas, G., Wolfbeis, O.S., Graw, M., 2012. The activity ratio of ^{228}Th to ^{228}Ra in bone tissue of recently deceased humans: a new dating method in forensic examinations. Anthropol. Anzeiger 69 (2), 147–157.